Longterm Culture of Telomerase-Transduced Rheumatoid Arthritis Fibroblast-like Synoviocytes Display a Distinct Gene Expression Pattern

YUBO SUN, GARY FIRESTEIN, DAVID BOYLE, HELEN GRUBER, and HERMAN CHEUNG

ABSTRACT. ***Objective.*** To extend the lifespan of rheumatoid arthritis fibroblast-like synoviocytes (RA FLS) using human telomerase catalytic subunit (hTERT) and to test the hypothesis that longterm culture of hTERT-RA FLS may display a disease-specific gene expression pattern.

Methods. RA 516 FLS were transduced by hTERT and the replicative properties of hTERT-RA 516 FLS were evaluated by repeated expansion. Gene expressions in hTERT-RA 516 FLS (passage 8) were compared with the gene expressions in hTERT-osteoarthritis (OA) 13A FLS (passage 8) by microarrays and RT-PCR. After continuous expansion in culture for an additional 4 months, gene expression was examined again using real-time RT-PCR and microarray.

Results. While primary RA 516 FLS stopped dividing after repeated culture for about 120 days, hTERT-RA 516 FLS continued to grow at a steady rate. The hTERT-RA 156 FLS displayed a distinct gene expression pattern different from hTERT-OA 13A FLS. Several putative autoantigens and cytokine A2/monocyte chemoattractant protein-1 were expressed at significantly higher levels in longterm culture of hTERT-RA 516 FLS.

Conclusion. Telomerase-transduced RA FLS offer an alternative cell model for the study of RA and for examination of cellular/genetic alterations in RA FLS. Our findings provide further support for the notion that RA FLS are altered cells. (First Release Sept 15 2007; J Rheumatol 2007;34:1959–70)

Key Indexing Terms:
SYNOVIOCYTES RHEUMATOID ARTHRITIS AUTOANTIGEN CCL2
CHI3L1 HAPLN1 AGC1 PRG4 TELOMERASE

Rheumatoid arthritis (RA) is an inflammatory disease characterized by severe abnormal immune response and progressive destruction of synovial joints. RA synovial tissue is characterized by intimal lining-layer hyperplasia and infiltration of the sublining by macrophages and T and B cells. The aggressive front of synovial tissue called pannus invades and destroys local articular structure. The pathogenesis of RA is still unclear; however, multiple pathways have been implicated including T cell-dependent abnormal immune response, T cell-independent cytokine network, and fibroblast-like synoviocyte (FLS)-dependent synovial hyperplasia[1-3]. Although the connections and the interplay between these multiple pathways are not fully understood, it is likely that they are not mutually exclusive, but rather intimately linked.

Considerable data have accumulated to support a role for a FLS-dependent pathway in RA synovial joint destruction. It has been shown that synovial hyperplasia is accompanied by the occurrence of FLS with a transformed-appearing phenotype[4] and that RA FLS proliferate in an anchorage-independent manner[5]. The most convincing evidence supporting a FLS-dependent pathway is the observation that FLS from patients with RA, but not FLS from patients with osteoarthritis (OA), maintain their invasive behavior in the absence of T cells and macrophages[6,7]. These observations indicate that RA FLS are altered cells and different from OA FLS.

One of the effective treatments for RA currently in use is the neutralization of tumor necrosis factor-α (TNF-α) using TNF-α-specific antibodies. However, many patients do not respond to this treatment[8]. Similarly, the response to methotrexate treatment also varies among patients with RA. These variances in responses to treatment indicate that RA is a heterogeneous disease. The heterogeneity of RA and the existence of multiple pathways of tissue destruction are further suggested by distinctly different gene expression profiles in RA synovium derived from different patients[9-12], and the interindividual differences in organization of infiltrated

From the Department of Orthopaedic Surgery, Carolinas Medical Center, Charlotte, North Carolina; the Division of Rheumatology, Allergy and Immunology, University of California San Diego, School of Medicine, La Jolla, California; and the Department of Biomedical Engineering, University of Miami, Coral Gables, Florida, Research Service and Geriatric Research, Education, and Clinical Center, Veterans Affairs Medical Center, Miami, Florida, USA.

Y. Sun, PhD; H.E. Gruber, PhD, Department of Orthopaedic Surgery, Carolinas Medical Center; G.S. Firestein, MD; D.L. Boyle, PhD, Division of Rheumatology, Allergy and Immunology, University of California San Diego, School of Medicine; H.S. Cheung, PhD, Department of Biomedical Engineering, University of Miami, Coral Gables, Florida, Research Service and Geriatric Research, Education, and Clinical Center, Veterans Affairs Medical Center, Miami.

Address reprint requests to Dr. Y. Sun, Department of Orthopaedic Surgery, Biology Division, Cannon Research 304, Carolinas Medical Center, Charlotte, NC 28232, USA.
E-mail: yubo.sun@carolinashealthcare.org

Accepted for publication June 29, 2007.

immune cells in RA synovium[13,14]. This heterogeneity of RA highlights the necessity to investigate individual patients and individual patient-derived FLS in depth in addition to large-scale analysis of RA FLS. Investigation of individual patient-derived FLS offers a complementary approach to determine the molecular basis underlying the heterogeneity of RA and the phenotypic or genetic differences between RA FLS derived from different patients or between RA FLS and OA FLS. Investigation of individual patient FLS may provide information for development of personalized treatment in the future.

Considerable efforts have been devoted to investigating the molecular basis and mechanism underlying the invasive phenotype of RA FLS. Many distinct gene expression patterns have been identified by analyzing gene expression profiles of cultured RA FLS[9-12]. However, cultured RA FLS of early passages may contain other cell types, including macrophages and dendritic cells, that may secrete inflammatory cytokines and express cell type-specific proteins. Primary cultured RA FLS (2–4 passages) used in many reported studies may contain up to 3% of other cell types. The gene expression profiles of RA FLS determined using primary RA FLS of early passages may reflect a gene expression profile in an "activated" stage and may not reflect an intrinsic characteristic or a stable trait of RA FLS themselves. Study of telomerase-immortalized RA FLS may eliminate such potential problems because the coexistence of other cell types in telomerase-immortalized FLS, especially in longterm culture, is highly unlikely. Given the potential importance of hTERT-RA FLS with a stable gene expression profile in RA research, we undertook this study to establish human telomerase-immortalized RA FLS and to test the hypothesis that longterm cultures of hTERT-RA FLS may display a disease-specific gene expression pattern that may reveal intrinsic characteristics or stable traits of RA FLS.

MATERIALS AND METHODS

Human telomerase retroviral expression plasmid pBabe-hTERT-hygromycin was a gift of Dr. R.A. Weinberg at the Massachusetts Institute of Technology[15]. Recombinant human interleukin 1ß (IL-1ß) and tumor necrosis factor-α (TNF-α) were obtained from R&D Systems (Minneapolis, MN, USA). Basic calcium phosphate (BCP) crystals were synthesized as described[16]. Dulbecco's modified Eagle's medium (DMEM), fetal bovine serum (FBS), and stock antibiotic/antimycotic mixture were from Invitrogen (Carlsbad, CA, USA).

Isolation and culture of FLS. RA 516 FLS were isolated by enzymatic dispersion of synovial tissues obtained from a 23-year-old female patient with RA. The synovial tissue was procured following a protocol approved by the Institutional Review Committee. Briefly, synovial tissue was minced and incubated with 1 mg/ml collagenase in serum-free DMEM for 2 h at 37°C, filtered through nylon mesh, extensively washed, and cultured in DMEM supplemented with 10% FBS, penicillin, streptomycin and L-glutamine in a humidified 5% CO_2 atmosphere. After overnight culture, nonadherent cells were removed, and adherent cells were cultured in DMEM plus 10% FBS. FLS (passages 2–4) were harvested and saved at –159°C until use.

Infection and selection of RA 516 FLS. We previously reported the immortalization of human OA 13A FLS using human telomerase. hTERT-OA 13A FLS was established by infection of human OA FLS derived from a female patient with OA with hTERT-expressing retrovirus and selected using hygromycin. Infection and selection of RA 516 FLS were carried out as described[17]. Briefly, 10 mg of pBabe-hTERT-hygromycin plasmid and control vector pBabe-hygromycin plasmid were transfected into amphotropic PT67 packaging cells (BD Biosciences, San Diego, CA, USA) using LipofectAmine (Invitrogen). Media containing hTERT-expressing retroviruses were collected from the virus-producing PT67 cells, filtered through a 0.45-µm filter, mixed with DMEM containing 8 µg/ml polybrene, and added to 75% confluent RA 516 FLS (passage 6) cultured in 100 mm plates. RA 516 FLS were infected for 1 day, then selected and expanded in culture medium containing 150 µg/ml hygromycin. When the stably transduced RA 516 FLS reached 75% confluence (5–6 weeks; passage 7), they were split and expanded. A portion of the hTERT-RA 516 FLS was harvested and saved at –159°C and another portion of the hTERT-RA FLS (passage 8) was used for characterization. RA 516 FLS stably transduced with pBabe-hTERT retrovirus was referred to as hTERT-RA 516 FLS and RA 516 FLS stably transduced with pBabe retrovirus was referred to as pBabe-RA 516 FLS.

Detection of telomerase activity. Telomerase activity was determined using the TRAPeze telomerase detection kit (Intergen Co., Purchase, NY, USA) according to the manufacturer's instructions. Briefly, 10^6 FLS (passage 8) were homogenized in 200 ml of CHAPS lysis buffer and incubated 30 min on ice. After incubation, the lysate was centrifuged at 12,000 g for 20 min at 4°C. An aliquot (48 µl) of the supernatant was mixed with the TRAPeze reaction mixture containing telomerase substrate primer (5'-AAT CCG TCG AGC AGA GTT-3'). Another aliquot of the supernatant was incubated at 85°C for 10 min to inactivate the telomerase before being mixed with the reaction mixture (as a negative control). After incubation at 30°C for 30 min, polymerase chain reaction (PCR) was performed with a 2-step cycle of 30 s at 94°C and 30 s at 59°C for 30 cycles. Reaction products were electrophoresed in 10% nondenaturing polyacrylamide gels. After electrophoresis, the gel was stained with ethidium bromide. Lysate prepared from hTERT-BJ1 human foreskin fibroblasts (BD Biosciences) was used as a positive control.

Assessment of proliferation, population-doubling, and morphology. Ten thousand hTERT-RA 516 FLS (passage 8) and primary RA 516 FLS (passage 6) were placed in 100-mm plates (triplicates) and cultured until 75% confluence (fresh medium was added every 3 days). The cells were then harvested and cell numbers counted in a hemocytometer. The population-doublings (PD) were calculated with the equation: $PD = \mathrm{Log}_{10}(N/N_0) \times 3.33$, where N = number of cells from 3 plates at the end of each experiment and N_0 = number of cells plated in the 3 plates at the beginning of each experiment. The average population-doubling time was calculated with the following equation: PD time = D/PD, where D = number of days cells were cultured in the experiment. The same experiment was repeated continuously until the primary RA 516 FLS ceased to proliferate. The morphology of primary RA 516 FLS and hTERT-RA 516 FLS was examined under a phase-contract microscope.

Semiquantitative reverse-transcription PCR. Total RNA samples were extracted from primary and hTERT-FLS using Trizol reagent (Invitrogen). Semiquantitative RT-PCR experiments were carried out using the ThermoScript RT-PCR System (Invitrogen). Briefly, 1 µg of RNA sample was reverse-transcribed at 60°C for 60 min, followed by enzyme inactivation at 85°C for 5 min. PCR experiments were carried out using gene-specific primers (Table 1). As an internal control, a 353-bp fragment of the housekeeping gene, ß-actin, was amplified. Amplifications were carried out for 25–40 cycles by denaturing at 95°C for 30 s, annealing at 55°C for 30 s, and extension at 72°C for 45 s, with a final extension at 72°C for 10 min. The products were electrophoresed on 2% agarose gels, stained with ethidium bromide, and photographed using a low-light image system (ChemiImager 4000, Alpha Innotech Corp., San Leandro, CA, USA). Each RT-PCR experiment was repeated at least 3 times using 2 or 3 different RNA batches.

Microarray experiments. hTERT-RA 516 FLS (passage 8) and hTERT-OA 13A FLS (passage 8) were plated in 100 mm plates at 70% confluence. Cell culture conditions were strictly followed in order to prevent experimentally induced gene expression changes. On the second day, fresh medium containing 10% serum was added and cells were cultured for 24 h. Total RNA was

Table 1. Gene-specific primers used for semiquantitative RT-PCR.

Gene	Primers
Egr-1	5'- AAC AGT GGC AAC ACC TTG TG-3'
	5'- ACT GGT AGC TGG TAT TGA GG-3'
MMP-1	5'-GAT CAT CGG GAC AAC TCT CCT-3'
	5'-TCC GGG TAG AAG GGA TTT GTG-3'
IGFBP3	5'-AGG ACA TGA CCA GCA GCT G-3'
	5'-CAC TGT ACG GGG AGT GGG-3'
Cyr61	5'-GTA TTA CAT TTC CCC TCC CTC-3'
	5'-TTC CAT CCC TTC CTG AAG G-3'
CTGF	5'-CTT GTG GCA AGT GAA TTT CC-3'
	5'-TGC TTT GAA CGA TCA GAC AA-3'
Nov	5'-CAC GGC GGT AGA GGG AGA TA-3'
	5'-GGG TAA GGC CTC CCA GTG AA-3'
AGC1	5'-CTG CAA CTG AAG TGC CC-3'
	5'-AGG CTG ATG GTT CCT CTG A-3'
PRG1	5'-ATT TTC CCA CCT TGA CAC CA-3'
	5'-ATG ATG TTG GTT GAA CAT GAT ACC-3'
PRG4	5'-CCT TAG ACT GAT GAG CAA AGG-3'
	5'-GAG CCA TGC AAT GGG AGG-3'
ESM1	5'-AAA TCC ACG CTG ATC CCG-3'
	5'-CAC CAT GCA TCA CAA TTT GG-3'
CCL2	5'-CCC CAC AGC TTA CAG ACC AT-3'
	5'-CAA GAG GAA AAG CAA TTT CCC-3'
OSF-2	5'-AGT TCT GGC TAA CTT TGG AAT CC-3'
	5'-TAA AAA ATA TGC ATT GCA AGA AGC-3'
PTX3	5'-AAC ACA TGC CAG TTG GG-3'
	5'-GAG TTT ATC TGA CAG AGA CAC AGC-3'
GREM1	5'-AAA TTC GCC TAG CGT GAG AA-3'
	5'-AGA ACC CTT GCA ACT CGA GA-3'
ß-actin	5'-GCT CGT CGT CGA CAA CGG CTC-3'
	5'-CAA ACA TGA TCT GGG TCA TCT TCT C-3'

extracted using Trizol reagent; RNA purification was performed using an Oligotex kit (Qiagen, Valencia, CA, USA) and the purified RNA was subjected to microarray experiments using Agilent human cDNA array B chips (Agilent Technologies, Palo Alto, CA, USA). Briefly, 10 µg of the RNA sample were mixed with 200 pmol oligo-dT primer. After 10 min incubation at 70°C and 5 min at 4°C, 20 units of Transcriptor reverse transcriptase (Roche, Indianapolis, IN, USA), 10 nmol of dents, and 4 mol of aminoallyl-dUTP (Ambion, Austin, TX, USA) were added, and this mixture was incubated 2 h at 42°C. After 30 min, the cDNA samples were purified using a QIAquick PCR purification kit (Qiagen). The cDNA samples were mixed with Cy3- or Cy5-NHS ethers and the labeled cDNA samples were purified using the QIAquick PCR purification kit before being hybridized to Agilent microarray gene chips. The microarray was scanned at 10-micron resolution using a GenePix 4000A scanner (Axon Instruments, Union City, CA, USA) and the image was analyzed using the GenePix Pro 5.1 software (Axon) for normalization and statistical analysis. Each array was normalized for signal intensities across the whole array and locally, using Lowess normalization (Lowess, Cleveland, OH, USA). Data were then filtered for unreliable datapoints (irregular geometry, scratched, S/N ratio < 3, and/or saturated signal) using Acuity software (Axon). Filtered data were imported into GeneSpring software for futher statistical analysis (Silicon Genetics, Redwood City, CA, USA). In order to eliminate dye bias, the microarray experiments were performed twice with reversed fluorescent labels. Finally, differentially expressed genes were classified according to the gene ontology category biological process using Onto-Express software (available from: http://vortex.cs.wayne.edu/Projects.html).

Real-time-PCR. hTERT-RA 516 FLS (passage 8) and hTERT-OA 13A FLS (passage 8) were continuously cultured for an additional 4 months. The longterm cultures of hTERT-RA 516 FLS (roughly passage 25) and hTERT-OA 13A FLS (roughly passage 25) were plated in 100 mm plates at 70% confluence. On the second day, fresh medium containing 10% serum was added and cells were cultured for 24 h. Total RNA samples were extracted using Trizol reagent and cDNA was synthesized using TaqMan® reverse transcription reagents (Applied Biosystems, Foster City, CA, USA). Quantitative RT-PCR was then performed. Briefly, quantification of relative transcript levels for cytokine A2/monocyte chemoattractant protein-1 (CCL2/MCP-1), chitinase 3-like 1/human cartilage glycoprotein-39 (CHI3L1/hc gp-39), cartilage link protein-1 (HAPLN1/Crtl1), aggrecan 1 (AGC1), preoteoglycan 4 (PRG4), and the housekeeping gene GAPDH in the cDNA samples was performed and analyzed using the ABI7000 Real-Time PCR machine (Applied Biosystems). We used TaqMan® gene expression assays (Applied Biosystems) that contain a FAM-MGB probe for fluorescent detection. cDNA samples were amplified with an initial Taq DNA polymerase activation step at 95°C for 10 min, followed by 40 cycles of denaturation at 95°C for 15 s and annealing at 60°C for 1 min. For each gene, Ct values were obtained in triplicates. To normalize for variation in RNA amounts and reverse transcription efficiencies, transcript levels of the housekeeping gene GAPDH were determined. Fold-change was calculated as described[18] after normalizing the expression of the gene of interest to GAPDH. Each RT-PCR experiment was repeated twice using 2 different RNA batches.

RESULTS

Telomerase activity. Telomerase activity in hTERT-RA 516 FLS (passage 8) was determined utilizing a PCR-based TRAP assay. CHAPS buffer (as a negative control) and the TSR8 template provided with the kit (as a positive control) were used according to the manufacturer's instructions (Figure 1, lanes 1 and 6, respectively), in addition to using the lysates prepared from a commercial telomerase-transduced human foreskin fibroblast cell line, BJ1, the pBabe-RA 516 FLS, and hTERT-RA 516 FLS. As shown in Figure 1, a high level of telomerase activity was detected in the BJ1 cells and hTERT-RA 516 FLS (lanes 2 and 4). In contrast, no telomerase activity was detected in pBabe-RA 516 FLS (lane 3) and the heat-treated lysate prepared from the hTERT-RA 516 FLS (lane 5).

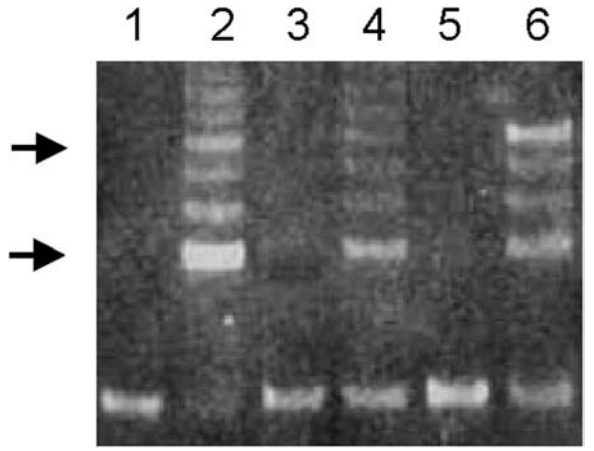

Figure 1. Telomerase activities. Telomeric-repeat amplification assay was performed to determine the telomerase activity. Lane 1: assay performed using CHAPS buffer (negative control); Lane 2: assay using cell extract prepared from hTERT-BJ1 cells (positive control); Lane 3: assay using cell extract prepared from pBabe-transduced RA 516 FLS; Lane 4: assay using cell extract prepared from hTERT-RA 516 FLS; Lane 5: assay using heat inactivated cell extract prepared from hTERT-RA 516 FLS; Lane 6: assay using TSR8 template (positive control).

Morphology, proliferation, and population-doublings. The morphology of hTERT-RA 516 FLS (passage 8; Figure 2A) is similar to the morphology of primary RA 516 FLS (passage 6; Figure 2B). The morphology of the longterm culture of hTERT-RA 156 FLS (passage 25) was also examined, shown together with the longterm culture of hTERT-OA 13A FLS (Figure 2C, 2D). No difference was observed between the morphology of passage 8 and the morphology of passage 25 hTERT-RA. These observations indicated that the expression of telomerase had little effect on the morphology of RA 516 FLS. The effects of telomerase transduction on the proliferation and population-doublings of RA 516 FLS were also examined. As shown in Figure 3A, the proliferative rate of the primary RA 516 FLS (passage 6) decreased with time and reached senescence after 100–120 days in culture (dotted line). In contrast, hTERT-RA 516 FLS maintained a steady proliferative rate and continued to grow (solid line). The hTERT-RA 516 FLS still maintained a steady proliferative rate after repeated expansion in culture for more than 400 days. It took an average of 2.5–3 days for the primary RA 516 FLS of early passage (passage 6) to double their numbers. It took a similar time (2.6 ± 0.4 days) for hTERT-RA 516 FLS to double their numbers (Figure 3B). These data indicate that hTERT-RA 516 FLS had a proliferative rate similar to that of primary RA 516 FLS of early passages. The previously established hTERT-OA 13A FLS used in this study had a similar proliferative rate. It took about 2.3 ± 0.4 days for hTERT-OA 13A FLS to double their numbers[17].

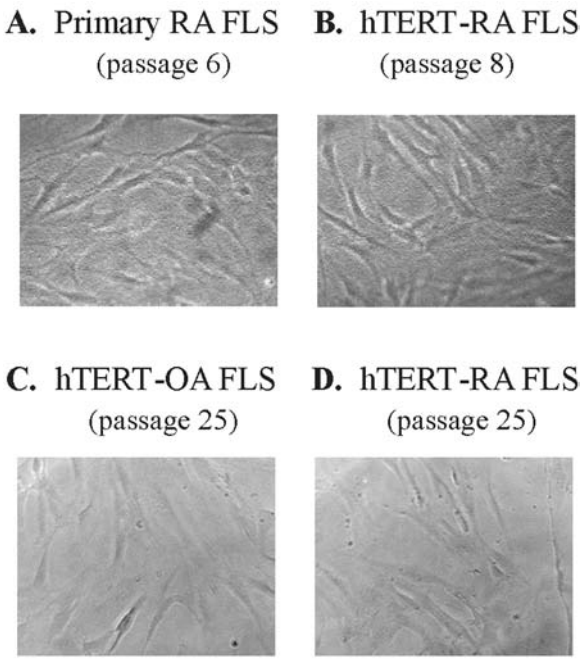

Figure 2. Morphology of primary RA 516 FLS and hTERT-RA 516 FLS. Primary RA 516 FLS (passage 6) and hTERT-RA 516 FLS (passage 8) were placed in 100-mm plates and grown until 60%–75% confluent. The morphology of these FLS was examined under microscopy. A. Primary RA 516 FLSs (passage 6). B. hTERT-RA 516 FLS (passage 8). Similarly, the morphology of passage 25 hTERT-OA 13A FLS and the morphology of passage 25 hTERT-RA 516 FLS was examined under microscopy. C. hTERT-OA 13A FLS. D. hTERT-RA 516 FLS.

A

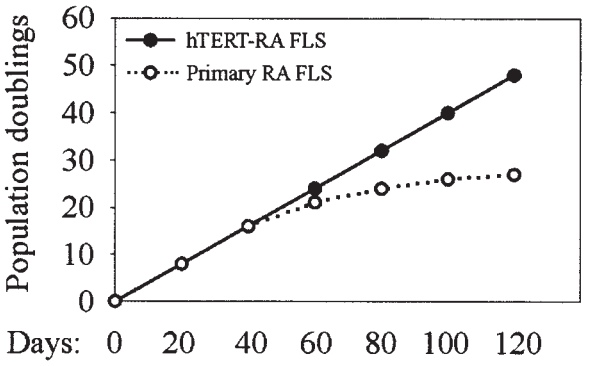

B

Experiment	hTERT-RA FLS	Primary RA FLS
1	2.6 days	2.3 days
2	2.3 days	2.6 days
3	2.7 days	3.2 days
4	2.8 days	5.8 days
5	2.6 days	16.5 days

Figure 3. Cell growth and doubling time. A. Proliferative behavior of hTERT-RA 516 FLS of passage 8 and the primary RA 516 FLS of passage 6 was followed for about 120 days. B. The average of population-doubling time of the RA FLS during the first 16 days (experiment 1), the following 18 days (experiment 2), additional 20 days (experiment 3), and additional 60 days (experiments 4 and 5).

Expression of early growth response-1 (egr-1). Egr-1 was the first gene reported to express spontaneously at a higher level in primary culture of RA FLS than in primary culture of OA FLS[19-21]. We examined the expression of *egr-1* in hTERT-RA 516 FLS (passage 8), primary RA 516 FLS (passage 6), and hTERT-OA 13A FLS (passage 8). As shown in Figure 4A, expression of *egr-1* in the hTERT-RA 516 FLS (lane 2) and the primary RA 516 FLS (lane 3) was about 3-fold higher than in hTERT-OA 13A FLS (lane 1). The RT-PCR experiment was repeated 3 times using different RNA batches. Similar results were always obtained. These results indicated that hTERT-RA 516 FLS (passage 8) maintained the characteristics of the primary untransduced RA 516 FLS (passage 6).

Expression of matrix metalloproteinases (MMP-1) after IL-1ß, TNF-α, and BCP crystal treatment. IL-1ß exists in RA synovial fluid and stimulates expression of MMP[22]. We ana-

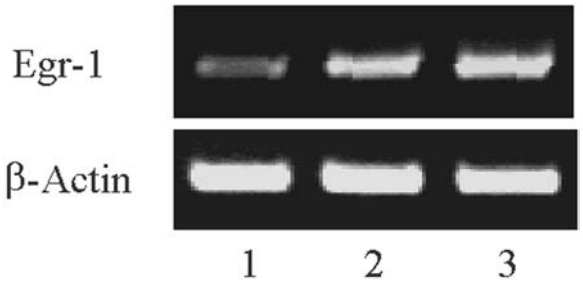

Figure 4. mRNA level of egr-1. hTERT-OA 13A FLS (lane 1), hTERT-RA 516 FLS (lane 2), and primary RA 516 FLS (lane 3) were plated in 60-mm plates at 75% confluence. On the second day, fresh medium containing 10% serum was added and cells were cultured another 24 h. Cells were then harvested and total RNA extracted. mRNA levels of egr-1 (28 cycles) and ß-actin (28 cycles) were examined by semiquantitative RT-PCR. Experiments were repeated at least 3 times and used 2 different RNA batches. Elevated expression of egr-1 was confirmed later by microarray experiments (Table 2).

lyzed the mRNA levels of MMP-1 before and after IL-1ß treatment. As shown in Figure 5A, expression of MMP-1 was stimulated by IL-1ß similarly in hTERT-RA 516 FLS (passage 8) and in primary RA 516 FLS (passage 6). We also analyzed the mRNA levels of MMP-1 before and after treatments with

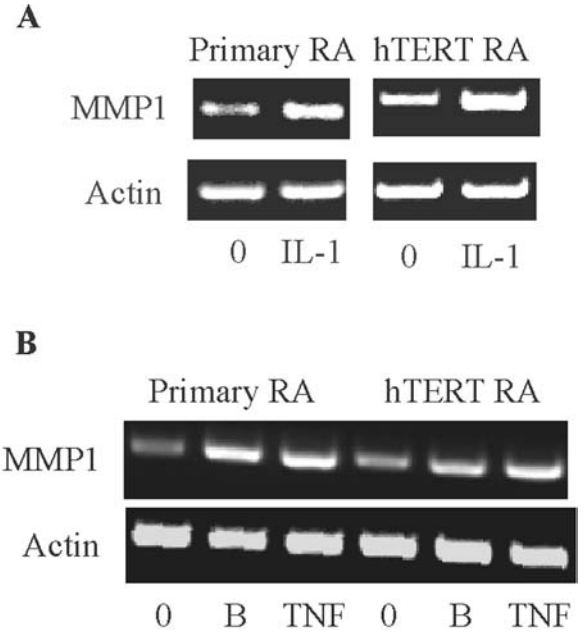

Figure 5. mRNA level of MMP1 before and after treatments (A). Primary RA 516 FLS (passage 6) and hTERT-RA 516 FLSs (passage 8) were plated in 60-mm plates at 75% confluence. On the second day, fresh medium without serum was added; 24 h later, half the cells were treated with 5 ng/ml IL-1ß in medium containing no serum and the other half were kept untreated (control). After 24 h, cells were harvested and total RNA extracted. mRNA levels of MMP1 (30 cycles) and ß-actin (25 cycles) were determined by semiquantitative RT-PCR (B). Similarly, primary RA 516 FLS and hTERT-RA 516 FLS were treated with 50 mg/ml BCP crystals or 1 ng/ml TNF-α in medium containing no serum for 24 h. mRNA levels of MMP1 (30 cycles) and ß-actin (30 cycles) were determined by semiquantitative RT-PCR. Experiments were repeated at least 3 times and used 2 different RNA batches.

TNF-α or BCP crystals. Again, the expression of MMP-1 was stimulated by TNF-α and BCP crystals similarly in hTERT-RA 516 FLS and in primary RA 516 FLS (Figure 5B). These results indicated that hTERT-RA 516 FLS preserved a similar sensitivity and response to external stimuli as that of the primary RA 516 FLS.

Microarray data. Since the above results indicated that hTERT-RA 516 FLS, similarly to hTERT-OA 13A FLS[17], maintained most of the characteristics of primary RA 516 FLS, we carried out a microarray analysis of hTERT-RA 516 FLS (passage 8) using hTERT-OA 13A FLS (passage 8) as a counterpart to test the hypothesis that hTERT-RA 516 FLS display a disease-specific gene expression pattern. Variation in hybridization caused by either the properties of the fluorescence or the labeling procedure was examined by reverse-labeling with Cy3 and Cy5. Only differences in the levels of gene expression varying more than 2-fold in both microarray experiments were taken to be significant. Among the 22,605 genes examined, a total of 234 genes were identified; 145 were expressed at higher levels and 89 at lower levels in hTERT-RA 516 FLS compared to hTERT-OA 13A FLS (data not shown). These differentially expressed genes were classified according to the gene ontology category biological process; selected genes are listed in Table 2.

Validation of differential expression of select genes by semiquantitative RT-PCR. We first carried out semiquantitative RT-PCR experiments to validate the differential expression of 4 genes that were classified into the functional family, regulation of cell growth (Table 2). They were insulin-like growth factor binding protein 3 (IGFBP-3), cysteine-rich angiogenic inducer 61 (CYR61/CCN1), connective tissue growth factor (CTGF/CCN2), and nephroblastoma overexpressed gene (NOV/CCN3). Elevated expressions of these 4 genes in hTERT-RA 516 FLS were confirmed (Figure 6A). We then carried out semiquantitative RT-PCR to validate differential expression of several extracellular matrix proteins including AGC1, PRG1, PRG4, and endothelial cell-specific molecule 1/dermatan sulfate proteoglycan (ESM1). The results are shown in Figure 6B. Besides these extracellular matrix proteins, 3 other genes reported to be highly expressed in RA synovial tissues were also examined: CCL2/MCP-1[9,23], osteoblast-specific factor 2 (OSF-2)[10], and pentaxin-related gene (PTX3)[24]. For comparison, gremlin (GREM1) was also examined. Semiquantitative RT-PCR confirmed the elevated expression of CCL2/MCP-1, OSF-2 and PTX3, and decreased expression of GREM1 (Figure 6C) in hTERT-RA 516 FLS compared to hTERT-OA 13A FLS. All experiments were performed at least 3 times and 2 different batches of RNA samples were used.

Longterm culture of hTERT-RA 516 FLS expressed higher level of putative autoantigens and CCL2/MCP-1. Examining the microarray data (Table 2), we found that several putative autoantigens were highly expressed in hTERT-RA 516 FLS compared to hTERT-OA 13A FLS. They were CHI3L/hc gp-

Table 2. Classification of select genes with increased expression in the hTERT-RA 516 FLS. The differential expression is the average of fold-difference from 2 microarrays.

Functional Family	Gene Name	Differential Expression (average of 2 arrays)	Human Accession no.	Description
Regulation of cell growth	IGFBP3	8.4	AK095408	Insulin-like growth factor binding protein 3, member of family of proteins that binds IGF1 and IGF2
	CYR61	5.2	BC016952	Cysteine-rich angiogenic inducer 61, a heparin-binding protein involved in cell adhesion, cell migration, angiogenesis, and cell proliferation
	IGFBP7	4.4	NM_001553	Insulin-like growth factor binding protein 7, member of family of proteins that binds IGF1 and IGF2
	CTGF	3.8	X78947	Connective tissue growth factor, an insulin like growth factor binding protein involved in apoptosis, angiogenesis, injury response, etc
	NOV	3.7	BC015028	Nephroblastoma overexpressed gene, an insulin-like growth factor binding protein, member of CCN family of growth regulators
	ESM1	3.6	BC011989	Endothelial cell-specific molecule 1, dermatan sulfate proteoglycan, involved in cell adhesion and proliferation
Cell proliferation	CYR61	5.2	BC016952	Cysteine-rich angiogenic inducer 61, a heparin binding protein involved in cell adhesion, cell migration, angiogenesis, and cell proliferation
	PRG4	4.3	U70136	Proteoglycan 4 (megakaryocyte-stimulating factor), a secreted proteoglycan with possible roles in regulating cell proliferation, ossification
	BCAT1	3.3	NM_005504	Cytosolic branched-chain amino acid aminotransferase (branched chain aminotransferase), reversibly transaminates branched-chain L-amino acids
	ERG	2.6	NM_004449	Homo sapiens v-ets erythroblastosis virus E26 oncogene-like (avian)
	FGF2	2.4	NM_002006	Basic fibroblast growth factor, regulates cell proliferation, differentiation, apoptosis, and migration in many tissues
	AKR1C3	–3.4	BC001479	Aldo keto reductase family 1 member C3, a type 2 3 alpha (17 beta)-hydroxysteroid dehydrogenase and member of the aldo keto reductase
	SERPINF1	–2.8	M76979	Pigment epithelium-derived factor, a neuroprotective protein that inhibits angiogenesis in the eye, regulates apoptosis
Regulation of cell cycle	FGF10	4.3	NM_004465	Homo sapiens fibroblast growth factor 10
	FGF2	2.4	NM_002006	Basic fibroblast growth factor, regulates cell proliferation, differentiation, apoptosis, and migration in many tissues
	HDAC9	2.3	NM_058176	Retired, was MEF2-interacting transcription repressor (histone deacetylase 7B, HDAC-related protein), a histone deacetylase-like protein
Response to stress	FGF10	4.3	NM_004465	Homo sapiens fibroblast growth factor 10
	MIG-6	3.9	AK096149	Mitogen-inducible gene 6, putative tumor suppressor expressed in a cell cycle-dependent manner, activates c jun N terminal kinase
	HSPB7	3.8	AK095911	Heat shock 27 kDa protein family member 7, may be involved in stress response, interacts with alpha filamin and actin binding protein 280
Inflammatory response	CCL2	4.4	M24545	Cytokine A2, CC chemokine that attracts monocytes, memory T-cells, natural killer cells and endothelial cells
	PTX3	2.8	BC039733	Pentaxin-related gene, a member of the pentaxin family of acute-phase proteins, may play roles in inflammation and bacterial defense
	CCL26	2.7	AF096296	Eotaxin-3, a CC class chemokine and chemoattractant for basophils, eosinophils, T cells, and monocytes, binds to CCR3
	HDAC9	2.3	NM_058176	Retired, was MEF2-interacting transcription repressor (histone deacetylase 7B, HDAC-related protein), a histone deacetylase-like protein
	AOX1	–4.4	L11005	Aldehyde oxidase, a molybdenum containing flavoenzyme involved in oxygen radical, xenobiotic, and drug metabolism
Cell adhesion	HAPLN1	8.0	U43328	Cartilage linking protein 1, an extracellular matrix protein that stabilizes aggrecan and hyaluronan aggregates in cartilage
	CYR61	5.2	BC016952	Cysteine-rich angiogenic inducer 61, a heparin-binding protein involved in cell adhesion, cell migration, angiogenesis, and cell proliferation
	AGC1	4.6	NM_013227	Aggrecan 1 (large aggregating chondroitin sulfate proteoglycan), component of cartilage
	CCL2	4.4	M24545	Cytokine A2, CC chemokine that attracts monocytes, memory T-cells, natural killer cells and endothelial cells
	THBS1	4.0	X04665	Thrombospondin-1, an extracellular matrix glycoprotein that interacts with other matrix proteins and cell-surface receptors
	POSTN	3.9	D13666	Osteoblast-specific factor 2, a putative cell adhesion molecule that may play a role in homophilic cell adhesion during bone formation

Table 2. Continued

Functional Family	Gene Name	Differential Expression (average of 2 arrays)	Human Accession no.	Description
	CTGF	3.8	X78947	Connective tissue growth factor, an insulin like growth factor binding protein involved in apoptosis, angiogenesis, injury response, etc
	LOC119587	3.8	BC036789	Protein with high similarity to adipocyte enhancer-binding protein 1 (mouse Aebp1), a transcriptional repressor
	PCDH1	3.7	NM_032420	Protocadherin 1, a cadherin-related cell adhesion molecule expressed in central nervous system and localizes to cell-cell contact
	CDH13	3.5	BC028624	Cadherin 13 (H cadherin), GPI-linked member of cadherin family of calcium-dependent adhesion molecules, mediates cell-cell interactions
	MFGE8	3.3	U58516	Milk fat globule-EGF factor 8 protein, a milk fat globule glycoprotein, protects against infection in breast-fed infants
	COL14A1	2.9	M64108	Protein containing 8 fibronectin type III domains and a von Willebrand factor type A domain
	DPT	2.8	NM_001937	Homo sapiens dermatopontin
	EDIL3	2.8	NM_005711	Homo sapiens EGF-like repeats and discoidin I-like domains 3
	JUP	2.4	NM_021991	Homo sapiens junction plakoglobin (JUP), transcript variant 2
	TNFRSF12A	2.3	AB035480	TNF receptor superfamily member 12A (TWEAK receptor), activates caspase-dependent apoptosis
	DSG2	–5.5	NM_001943	Desmoglein 2, a cadherin-related adhesive glycoprotein found in desmosomes (cell-cell junctions)
	CD36	–5.0	M98398	CD36 antigen, an integral membrane receptor, binds thrombospondin, collagen, oxidized low density lipoprotein, long-chain fatty acids
	DSG3	–4.2	M76482	Desmoglein 3, cadherin superfamily member, forms the core of desmosomes, binds plakoglobin, maintains keratinocyte cell-cell adhesion
	EMILIN2	–3.2	NM_032048	Extracellular glycoprotein EMILIN-2, a secreted glycoprotein, contains a globular C1q domain and a cysteine-rich EMI domain
	ENTPD1	–2.8	NM_001776	Ectonucleoside triphosphate diphosphohydrolase 1, an integral membrane ectoapyrase that hydrolyzes extracellular ATP and ADP to AMP
	LSAMP	–2.2	NM_002338	Homo sapiens limbic system-associated membrane protein
Cell-cell signaling	FGF10	4.3	NM_004465	Homo sapiens fibroblast growth factor 10
	FGF2	2.4	NM_002006	Basic fibroblast growth factor, regulates cell proliferation, differentiation, apoptosis, and migration in many tissues
	PENK	6.2	NM_006211	Homo sapiens proenkephalin
	CCL26	2.7	AF096296	Eotaxin-3, a CC class chemokine and chemoattractant for basophils, eosinophils, T cells, and monocytes, binds to CCR3
	PCDH1	3.7	NM_032420	Protocadherin 1, a cadherin-related cell adhesion molecule expressed in the CNS and localizes to cell-cell contact
	CCL2	4.4	M24545	Cytokine A2, CC chemokine that attracts monocytes, memory T-cells, natural killer cells and endothelial cells
	MME	–3.1	J03779	Neutral endopeptidase (neprilysin, enkephalinase), an integral membrane metalloendopeptidase that cleaves and inactivates regulatory peptides
	ENTPD1	–3.3	NM_001776	Ectonucleoside triphosphate diphosphohydrolase 1, an integral membrane ectoapyrase that hydrolyzes extracellular ATP and ADP to AMP
	IL7	–7.8	J04156	Interleukin 7, a hematopoietic growth factor required for normal growth and development of B cells and T cells
Intracellular signaling cascade	JAK3	5.5	U09607	Janus kinase 3, a tyrosine kinase activated by interleukins IL2, IL4, IL9, and IL13, serves in T cell activation
	TXK	4.4	NM_003328	Homo sapiens TXK tyrosine kinase
	PARG1	3.4	U90920	PTPL1 associated RhoGAP 1, a GTPase- activating protein for the Rho sub family of ras-related GTP-binding proteins
	ADCY3	–3.0	NM_004036	Adenylyl cyclase 3, a membrane-associated ATP to cAMP-converting enzyme inhibited by Ca2+/calmodulin-dependent protein kinase II
Regulation of transcription	PCDH1	3.7	NM_032420	Protocadherin 1, a cadherin-related cell adhesion molecule expressed in the CNS and localizes to cell-cell contact
	GAS41	3.4	U61384	Glioma-amplified sequence 41, putative transcription factor essential in cell proliferation, resembles AF-9 (MLLT3) and ENL (MLLT1)
	IRF6	2.9	AF027292	Interferon regulatory factor 6, a transcription factor that regulates expression of members of interferon alpha and beta family
	GSC	2.9	AY177407	Goosecoid, a member of the homeodomain family of transcription factors

Table 2. Continued

Functional Family	Gene Name	Differential Expression (average of 2 arrays)	Human Accession no.	Description
	ERG	2.6	NM_004449	Homo sapiens v-ets erythroblastosis virus E26 oncogene-like (avian) (ERG)
	MID1	2.5	AF269101	Midline 1, member of the B-box family of RING finger proteins that associates with microtubules and plays a role in body axis patterning
	HDAC9	2.3	NM_058176	Retired, was MEF2-interacting transcription repressor (histone deacetylase 7B, HDAC-related protein), a histone deacetylase-like protein
	MAFB	2.2	NM_005461	Homo sapiens v-maf musculoaponeurotic fibrosarcoma oncogene homolog B (avian)
	ZNF593	2.2	BC002580	LOC51042 (hT86), has transcriptional repressor activity, inhibits DNA binding activity and transcriptional repression activity of Oct-2
	EGR1	2.2	M62829	Early growth response 1, an early response protein, a zinc finger transcription factor
	LOC127540	–2.8	AK097707	Protein with high similarity to high mobility group (nonhistone chromosomal) protein 2 (rat Hmgb2), which binds and bends DNA
	SHOX	–2.1	U89331	Short stature homeobox, a homeodomain containing transcription activator involved in skeletal development
Metabolism	CPE	2.9	X51405	Carboxypeptidase E, a metalloprotease involved in processing of bioactive peptides and neurotransmitters including insulin
	CHI3L1	2.7	BC008568	Chitinase 3-like 1 (cartilage glycoprotein 39), binds chitin but does not have chitinase activity, associated with RA
	PSAT1	3.0	BC004863	Phosphoserine aminotransferase, a member of the aminotransferases class-V family of pyridoxalphosphate-dependent enzymes
	BCAT1	3.3	NM_005504	Cytosolic branched-chain amino acid aminotransferase (branched chain aminotransferase), reversibly transaminates branched-chain L-amino acids
	SLC27A5	2.2	AF064255	Very long-chain Acyl-CoA synthetase related, catalyzes the conversion of cholic acid to choloyl-CoA
	ALDH1A3	4.8	U07919	Aldehyde dehydrogenase 1 family member A3, a retinaldehyde dehydrogenase that catalyzes the oxidation of all-trans-retinaldehyde to retinoic
	CES1	–3.4	L07764	Carboxylesterase 1 (monocyte-macrophage serine esterase 1), hydrolyzes aromatic and aliphatic esters
	HSD11B1	–11.0	BC012593	11-beta-hydroxysteroid dehydrogenase type 1, catalyzes the interconversion of inactive cortisone and active cortisol
Skeletal development	TNFRSF11B	4.1	BC030155	Osteoprotegerin, soluble member of TNF receptor superfamily that may act as a secreted decoy receptor
	POSTN	3.9	D13666	Osteoblast-specific factor 2, a putative cell adhesion molecule, may play a role in homophilic cell adhesion during bone formation
	COL1A1	2.9	BC036531	Alpha 1 subunit of type I collagen, a structural constituent of bone, involved in skeletal development and epidermal differentiation
	SHOX	–2.1	U89331	Short stature homeobox, a homeodomain containing transcription activator involved in skeletal development
Electron transport	FLJ23153	5.9	NM_024636	Member of the NADP oxidoreductase coenzyme F420-dependent family
	C10orf33	5.0	BC006131	Protein of unknown function, has high similarity to uncharacterized C. elegans F37C4.6
	NOX5	3.7	AF317889	NADPH oxidase EF hand calcium-binding domain 5, calcium-dependent NADPH oxidase and hydrogen ion transporter
	CYP2A6	2.5	M33318	Nicotine C-oxidase (cytochrome P450 2A6), functions in oxidizing precarcinogens and drugs, including nitrosamine activation, nicotine
	PTGIS	2.2	D38145	Prostaglandin I2 (prostacyclin) synthase, a member of the cytochrome P450 family of proteins, converts prostaglandin H2 to the vasodilator
	AOX1	–3.1	L11005	Aldehyde oxidase, a molybdenum containing flavoenzyme involved in oxygen radical, xenobiotic, and drug metabolism
	XDH	–2.4	NM_000379	Retired, was xanthine dehydrogenase, catalyzes oxidation of xanthine to uric acid in purine catabolism

39[25-27], HAPLN1/Crtl1[28,29], AGC1[30-32], and PRG4[33]. In addition, CCL2/MCP-1, an important chemokine molecule implicated in RA for attracting monocytes/microphages, memory T cells, natural killer cells, and endothelial cells[34-36], was also highly expressed in hTERT-RA 516 FLS. To determine whether the higher levels of expression of these putative

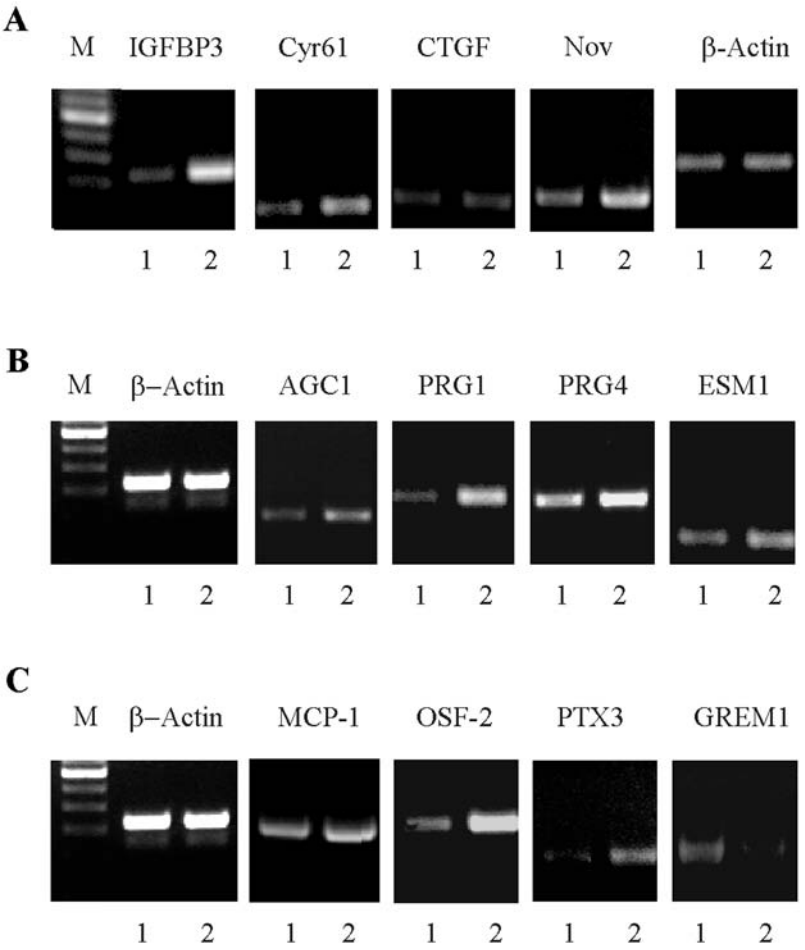

Figure 6. Validation of differential expression of select genes using semiquantitative RT-PCR. hTERT-OA 13A FLS (lane 1) and hTERT-RA 516 FLS (lane 2) were plated in 100-mm plates at 75% confluence. On the second day, medium containing 10% serum was added and cells were cultured another 24 h. RNA samples were then extracted and examined by semiquantitative RT-PCR. A. mRNA levels of IGFBP3 (25 cycles), Cyr61 (40 cycles), CTGF (35 cycles), Nov (28 cycles), and ß-actin (22 cycles). B. mRNA levels of AGC1 (30 cycles), PRG1 (28 cycles), PRG4 (28 cycles), ESM1 (40 cycles), and ß-actin (28 cycles). C. The mRNA levels of MCP-1 (30 cycles), OSF-2 (25 cycles), PTX3 (28 cycles), GREM1 (35 cycles), and ß-actin (28 cycles). Experiments were repeated at least 3 times and used 3 different RNA batches. Similar results were always obtained.

autoantigens and the CCL2/MCP-1 molecule reflected a stable trait of hTERT-RA 516 FLS, we examined the expression of these genes again using quantitative RT-PCR after repeated culture of hTERT-RA 516 FLS and hTERT-OA 13A FLS for an additional 4 months. The longterm cultured hTERT-RA 516 FLS (roughly passage 25) and hTERT-OA 13A FLS (roughly passage 25) were replated in 100 mm plates at 70% confluence and cultured for another 36 h before total RNA was extracted. Quantitative RT-PCR was then performed. Indeed, RT-PCR revealed that longterm culture of hTERT-RA 516 FLS expressed these putative autoantigens and CCL2/MCP-1 molecule at significantly higher levels in hTERT-RA 156 FLS compared to TERT-OA 13A FLS (Table 3). All experiments were performed twice (triplicates) and 2 different batches of RNA samples were used.

DISCUSSION

We report the successful transfer of hTERT and immortalization of RA 516 FLS. The hTERT-RA 516 FLS have grown in culture more than 400 days and maintain a steady growth rate. Similar to primary RA 516 FLS, hTERT-RA 516 FLS responded to IL-1ß, TNF-α, and BCP crystals with the induction of MMP1. In addition, hTERT-RA 516 FLS (passage 8) and the primary RA 516 FLS (passage 6) expressed a higher level of EGR-1 compared to hTERT-OA 13A FLS. These results together indicate that hTERT-RA 516 FLS (passage 8) maintained the characteristics of their parental primary RA 516 FLS (passage 6).

Our microarray data demonstrated that hTERT-RA 516 FLS displayed a distinct gene expression pattern compared to hTERT-OA 13A FLS. The genes that had an elevated expres-

Table 3. Microarray fold-changes (RA/OA) versus real-time-PCR fold-changes (RA/OA).

Gene	Microarray (passage 8 hTERT-FLS), Fold	Real-time-PCR (passage 25 hTERT-FLS), Fold	Microarray (passage 25 hTERT-FLS), Fold
CH13L1	2.7	2.5	3.8
HAPLN1	8.1	70.0	97.0
PRG4	4.3	2.9	3.8
AGC1	4.6	5.6	9.9
CCL2/MCP-1	4.4	3.0	4.8

sion in hTERT-RA 516 FLS preferentially participated in a limited number of functions (Table 2). Of the 6 differentially expressed genes classified into the functional family, regulation of cell growth, all 6 genes had elevated expression in hTERT-RA 516 FLS; of the 5 differentially expressed genes classified into the functional family, inflammatory response, 4 genes had an elevated expression; of the 22 differentially expressed genes classified into the functional family, cell adhesion, 16 genes had an elevated expression; of the 12 differentially expressed genes involved in regulation of transcription, 10 genes had an elevated expression. The distinct distribution of differentially expressed genes suggests that RA 516 FLS may display a defined cellular activity different from that of OA 13A FLS. Many of our findings were consistent with previous data reported from other laboratories including the elevated expression of CCL2/MCP-1[9], EGR-1[19], and PTX3[24] in RA FLS.

It has recently been reported that there is a significant increase in insulin-like growth factor binding protein 5 (IGFBP-5) in a subgroup of RA FLS[12]. We found no differential expression of IGFBP-5 in hTERT-RA 516 FLS compared to hTERT-OA 13A FLS. We observed an increase in the expression of IGFBP-3 and IGFBP-7 in the hTERT-RA 516 FLS (Table 2). We also observed an increase in the expression of Cyr61/CCN1, CTGF/CCN2, and Nov/CCN3. The CCN family comprises 6 members (CCN1 to 6) and CCN proteins have emerged as major regulators of angiogenesis, chondrogenesis, and fibrogenesis[37-40]. Although CCN proteins are distinct from members of the IGFBP superfamily, each member of the CCN family consists of 4 conserved cysteine-rich modular domains with sequence similarity to the IGFBP. The CCN family of proteins may bind to IGF and affect their functions. The elevated expression of IGFBP and CCN suggests that IGF-related signaling pathways may be altered in hTERT-RA 516 FLS.

Many putative autoantigens have been implicated in RA including CHI3L1/hc gp-39[25-27,41,42], HAPLN1/Crtl1[28,29], AGC1[30-32,43,44], PRG4[33], and type II collagen[45]. It is generally believed that these putative autoantigens are generated from articular cartilage. Interestingly, our study indicates that many of these putative autoantigens or cartilage-associated extracellular matrix proteins are expressed at higher levels in hTERT-RA 516 FLS compared to hTERT-OA 13A FLS. These results suggest that RA FLS may play a role in the elevated production of putative autoantigens observed in RA.

Another important finding is that both the short-term and longterm cultures of hTERT-RA 516 FLS express CCL2/MCP-1 at a significantly higher level than hTERT-OA 13A FLS. Our findings are consistent with a report that CCL2/MCP-1 is one of only 4 genes that encoded for cytokines, and chemokines are highly expressed in primary RA FLS compared to primary OA FLS[9]. This consistency between our findings and those of Cagnard, *et al*[9] again provides strong support for our hypothesis that telomerase-immortalized RA FLS maintain the characteristics of primary RA FLS and may display a disease-specific gene expression pattern. Because the coexistence of other cell types is highly unlikely in longterm culture of hTERT-RA 516 FLS, our findings suggest that the elevated expression of CCL2/MCP-1 and putative autoantigens reflects an intrinsic trait of RA 516 FLS. The elevated expression of CCL2/MCP-1 in RA FLS may play a role in attracting monocytes/macrophages and contribute to synovial hyperplasia.

Recently, we carried out another microarray experiment to examine the differential expressions between longterm culture of hTERT-RA 516 FLS (passage 25) and hTERT-OA 13A FLS using Affymetrix HG-U133_Plus_2 gene chip. Among the 72 genes listed in Table 2, 48 (67%) displayed similar differential expressions in the longterm culture of hTERT-RA 516 FLS and hTERT-OA 13A FLS detected by the Affymetrix HG-U133_Plus_2 gene chip (data not shown). Elevated expressions of the putative autoantigens CHI3L1/hc gp-39, HAPLN1/Crtl1, AGC1, PRG4, and the chemokine molecule CCL2/MCP-1 were again detected (Table 3). These results demonstrate that longterm cultures of hTERT-RA 516 FLS maintain a stable gene expression pattern. Among the other 24 genes listed in Table 2, 6 including CCL26, JUP, LSAMP, TXK, CYP2A6, and XDH showed opposite results. These 6 genes were found to have elevated expressions in passage 8 hTERT-RA 516 FLS using the Agilent human cDNA array B chip, but had decreased expression in passage 25 hTERT-RA 516 FLS using the Affymetrix HG-U133_Plus_2 gene chip. The other 18 genes including MIG-6, HSPB7, HDAC9, POSTN, LOC119587, PCDH1, COL14A1, PCDH1, JAK3, PARG1, GAS41, GSC, EGR1, LOC127540, CPE, SLC27A5, COL1A1, and C10orf33 displayed no differential expressions in passage 25 hTERT-RA 156 FLS and passage 25 hTERT-OA 13A FLS.

The different results between the first and the second microarray for the 24 genes may be attributed to several factors. The first is the different designs of the Agilent and Affymetrix gene chips. For example, JAK3 was detected using the Agilent gene chip, but it could not be confirmed by RT-PCR (data not shown), and it was not detected using the Affymetrix gene chip. The second factor may be the state of hTERT-RA 516 FLS. For example, both *osf-2* and *egr-1* were detected in the first microarray using the Agilent gene chip and the differential expressions of the 2 genes in the passage 8 hTERT-RA 516 FLS and hTERT-OA 13A FLS were confirmed by RT-PCR, but no differential expressions of the 2 genes were detected in passage 25 hTERT-RA 516 FLS and passage 25 hTERT-OA 13A FLS using the Affymetrix gene chip. This phenomenon is likely associated with the state of RA FLS. In early passage RA-FLS, RA FLS are in an "activated stage" and the activation is gradually diminished with each additional passage. It has been reported that RA synovial cells (passage 1) injected into nude mice become organized into a pannus-like structure, but no pannus-like structure was formed if later-passage synovial cells were used[46]. A third possibility is that the differences between the chips' results are due to random chance.

Our study has limitations; for example, all gene expressions were examined at transcription levels. In order to draw more definitive conclusions, confirmation at the protein level is needed. Another limitation is that gene expressions were compared between one telomerase-immortalized RA FLS and one telomerase-immortalized OA FLS. Although many of our findings are consistent with data reported from other laboratories where a large number of primary RA FLS and OA FLS were used, it is still uncertain how many and which of the differentially expressed gens listed here (Table 2) are disease-specific rather than individual-specific. It is also unclear whether longterm culture of RA FLS can be classified into different subgroups according to their gene expression profiles. A much larger number of telomerase-immortalized RA and OA FLS samples are needed to determine the disease-specific differential gene expressions or classify RA FLS into subgroups. We are establishing a larger number of telomerase-immortalized RA and OA FLS and will carry out further studies to address these limitations using these FLS lines.

We have successfully transduced and extended the lifespan of RA 516 FLS by exogenous-expressing human telomerase. The hTERT-RA 516 FLS display a distinct gene expression pattern and may provide an important tool for the study of disease markers, genetic or cellular alterations, and gene regulation in RA. It is unclear whether the elevated expression of putative autoantigens and CCL2/MCP-1 in RA FLS is a general feature of RA-derived FLS and may represent one of the missing links between the FLS-dependent synovial hyperplasia pathway and other pathways; this subject warrants further study.

REFERENCES

1. Firestein GS. Evolving concepts of rheumatoid arthritis. Nature 2003;423:356-61.
2. Goronzy JJ, Weyand CM. T-cell regulation in rheumatoid arthritis. Curr Opin Rheumatol 2004;16:212-7.
3. Muller-Ladner U. T cell-independent cellular pathways of rheumatoid joint destruction. Curr Opin Rheumatol 1995;7:222-8.
4. Fassbender HG. Histomorphological basis of articular cartilage destruction in rheumatoid arthritis. Collagen Rel Res 1983;3:141-55.
5. Lafyatis R, Remmers EF, Roberts AB, Yocum DE, Sporn MB, Wilder RL. Anchorage-independent growth of synoviocytes from arthritic and normal joints. Stimulation by exogenous platelet-derived growth factor and inhibition by transforming growth factor-beta and retinoids. J Clin Investigat 1989;83:1267-76.
6. Muller-Ladner U, Kriegsmann J, Franklin BN, et al. Synovial fibroblasts of patients with rheumatoid arthritis attach to and invade normal human cartilage when engrafted into SCID mice. Am J Pathol 1996;149:1607-15.
7. Wang AZ, Wang JC, Fisher GW, Diamond HS. Interleukin-1-beta-stimulated invasion of articular cartilage by rheumatoid synovial fibroblasts is inhibited by antibodies to specific integrin receptors and by collagenase inhibitors. Arthritis Rheum 1997;40:1298-307.
8. Feldmann M, Maini RN. Anti-TNF alpha therapy of rheumatoid arthritis: what have we learned? Annu Rev Immunol 2001;19:163-96.
9. Cagnard N, Letourneur F, Essabbani A, et al. Interleukin-32, CCL2, PF4F1 and GFD10 are the only cytokine/chemokine genes differentially expressed by in vitro cultured rheumatoid and osteoarthritis fibroblast-like synoviocytes. Eur Cytokine Netw 2005;16:289-92.
10. van der Pouw Kraan TC, van Gaalen FA, Huizinga TW, Pieterman E, Breedveld FC, Verweij CL. Discovery of distinctive gene expression profiles in rheumatoid synovium using cDNA microarray technology: evidence for the existence of multiple pathways of tissue destruction and repair. Genes Immun 2003;4:187-96.
11. Devauchelle V, Marion S, Cagnard N, et al. DNA microarray allows molecular profiling of rheumatoid arthritis and identification of pathophysiological targets. Genes Immun 2004;5:597-608.
12. Kasperkovitz PV, Timmer TC, Smeets TJ, et al. Fibroblast-like synoviocytes derived from patients with rheumatoid arthritis show the imprint of synovial tissue heterogeneity: evidence of a link between an increased myofibroblast-like phenotype and high-inflammation synovitis. Arthritis Rheum 2005;52:430-41.
13. Takemura S, Braun A, Crowson C, et al. Lymphoid neogenesis in rheumatoid synovitis. J Immunol 2001;167:1072-80.
14. Shi K, Hayashida K, Kaneko M, et al. Lymphoid chemokine B cell-attracting chemokine-1 (CXCL13) is expressed in germinal center of ectopic lymphoid follicles within the synovium of chronic arthritis patients. J Immunol 2001;166:650-5.
15. Meyerson M, Counter CM, Eaton EN, et al. hEST2, the putative human telomerase catalytic subunit gene, is up-regulated in tumor cells and during immortalization. Cell 1997;90:785-95.
16. McCarthy GM, Mitchell PG, Cheung HS. The mitogenic response to stimulation with basic calcium phosphate crystals is accompanied by induction and secretion of collagenase in human fibroblasts. Arthritis Rheum 1991;34:1021-30.
17. Sun Y, Firestein GS, Wenger L, Huang CY, Cheung HS. Telomerase-transduced osteoarthritic fibroblast-like synoviocyte cell line. Biochem Biophys Res Commun 2004;323:1287-92.
18. Pfaffl MW. A new mathematical model for relative quantification in real-time RT-PCR. Nucl Acids Res 2001;29:e45.

19. Trabandt A, Aicher WK, Gay RE, Sukhatme VP, Fassbender HG, Gay S. Spontaneous expression of immediately-early response genes c-fos and egr-1 in collagenase-producing rheumatoid synovial fibroblasts. Rheumatol Int 1992;12:53-9.
20. Aicher WK, Heer AH, Trabandt A, et al. Overexpression of zinc-finger transcription factor Z-225/Egr-1 in synoviocytes from rheumatoid arthritis patients. J Immunol 1994;152:5940-8.
21. Grimbacher B, Aicher WK, Peter HH, Eibel H. Measurement of transcription factor c-fos and EGR-1 mRNA transcription levels in synovial tissue by quantitative RT-PCR. Rheumatol Int 1997;17:109-12.
22. Jeong JG, Kim JM, Cho H, Hahn W, Yu SS, Kim S. Effects of IL-1-beta on gene expression in human rheumatoid synovial fibroblasts. Biochem Biophys Res Commun 2004;324:3-7.
23. Koch AE, Kunkel SL, Harlow LA, et al. Enhanced production of monocyte chemoattractant protein-1 in rheumatoid arthritis. J Clin Invest 1992;90:772-9.
24. Luchetti MM, Piccinini G, Mantovani A, et al. Expression and production of the long pentraxin PTX3 in rheumatoid arthritis. Clin Exp Immunol 2000;119:196-202.
25. Johansen JS, Stoltenberg M, Hansen M, et al. Serum YKL-40 concentrations in patients with rheumatoid arthritis: relation to disease activity. Rheumatology Oxford 1999;38:618-26.
26. Matsumoto T, Tsurumoto T. Serum YKL-40 levels in rheumatoid arthritis: correlations between clinical and laborarory parameters. Clin Exp Rheumatol 2001;19:655-60.
27. Vos K, Miltenburg AM, van Meijgaarden KE, et al. Cellular immune response to human cartilage glycoprotein-39 (HC gp-39)-derived peptides in rheumatoid arthritis and other inflammatory conditions. Rheumatology Oxford 2000;39:1326-31.
28. Guerassimov A, Zhang Y, Banerjee S, et al. Autoimmunity to cartilage link protein in patients with rheumatoid arthritis and ankylosing spondylitis. J Rheumatol 1998;25:1480-4.
29. Doran MC, Goodstone NJ, Hobbs RN, Ashton BA. Cellular immunity to cartilage link protein in patients with inflammatory arthritis and non-arthritic controls. Ann Rheum Dis 1995;54:466-70.
30. Li NL, Zhang DQ, Zhou KY, et al. Isolation and characteristics of autoreactive T cells specific to aggrecan G1 domain from rheumatoid arthritis patients. Cell Res 2000;10:39-49.
31. Glant TT, Mikecz K. Proteoglycan aggrecan-induced arthritis: a murine autoimmune model of rheumatoid arthritis. Methods Mol Med 2004;102:313-38.
32. Berlo SE, Guichelaar T, Ten Brink CB, et al. Increased arthritis susceptibility in cartilage proteoglycan-specific T cell receptor-transgenic mice. Arthritis Rheum 2006;54:2423-33.
33. Berthelot JM. Could rheumatoid arthritis result from an abnormal T cell response towards lubricin/superficial zone protein? Med Hypotheses 2004;62:894-7.
34. Harigai M, Hara M, Yoshimura T, Leonard EJ, Inoue K, Kashiwazaki S. Monocyte chemoattractant protein-1 (MCP-1) in inflammatory joint diseases and its involvement in the cytokine network of rheumatoid synovium. Clin Immunol Immunopathol 1993;69:83-91.
35. Ellingsen T, Buus A, Stengaard-Pedersen K. Plasma monocyte chemoattractant protein 1 is a marker for joint inflammation in rheumatoid arthritis. J Rheumatol 2001;28:41-6.
36. Taylor PC, Peters AM, Paleolog E, et al. Reduction of chemokine levels and leukocyte traffic to joints by tumor necrosis factor alpha blockade in patients with rheumatoid arthritis. Arthritis Rheum 2000;43:38-47.
37. Brigstock DR. Regulation of angiogenesis and endothelial cell function by connective tissue growth factor (CTGF) and cysteine-rich 61 (CYR61). Angiogenesis 2002;5:153-65.
38. Lin CG, Chen CC, Leu SJ, Grzeszkiewicz TM, Lau LF. Integrin-dependent functions of the angiogenic inducer NOV (CCN3): implication in wound healing. J Biol Chem 2005;280:8229-37.
39. Nishida T, Kubota S, Kojima S, et al. Regeneration of defects in articular cartilage in rat knee joints by CCN2 (connective tissue growth factor). J Bone Miner Res 2004;19:1308-19.
40. Yu C, Le AT, Yeger H, Perbal B, Alman BA. NOV (CCN3) regulation in the growth plate and CCN family member expression in cartilage neoplasia. J Pathol 2003;201:609-15.
41. Baeten D, Boots AM, Steenbakkers PG, et al. Human cartilage gp-39+, CD16+ monocytes in peripheral blood and synovium: correlation with joint destruction in rheumatoid arthritis. Arthritis Rheum 2000;43:1233-43.
42. Steenbakkers PG, Baeten D, Rovers E, et al. Localization of MHC class II/human cartilage glycoprotein-39 complexes in synovia of rheumatoid arthritis patients using complex-specific monoclonal antibodies. J Immunol 2003;170:5719-27.
43. Hanyecz A, Bardos T, Berlo SE, et al. Induction of arthritis in SCID mice by T cells specific for the "shared epitope" sequence in the G3 domain of human cartilage proteoglycan. Arthritis Rheum 2003;48:2959-73.
44. Zou J, Zhang Y, Thiel A, et al. Predominant cellular immune response to the cartilage autoantigenic G1 aggrecan in ankylosing spondylitis and rheumatoid arthritis. Rheumatology Oxford 2003;42:846-55.
45. Cook AD, Rowley MJ, Mackay IR, Gough A, Emery P. Antibodies to type II collagen in early rheumatoid arthritis. Correlation with disease progression. Arthritis Rheum 1996;39:1720-7.
46. Brinckerhoff CE, Harris ED Jr. Survival of rheumatoid synovium implanted into nude mice. Am J Pathol 1981;103:411-9.